RSC Advances

PAPER

View Article Online
View Journal | View Issue

Cite this: *RSC Adv.*, 2026, **16**, 12806

Computational analysis of umami and bitter taste interactions: orthogonality in receptor–ligand binding

Sergey Shityakov, *[ab] Samson Olusegun Afolabi, [a] Mariia S. Ashikhmina, [a] Ekaterina V. Skorb [a] and Michael Nosonovsky *[c]

We investigated the *in silico* binding of ligands relevant to the bitter taste in wine (flavan-3-ol) and the umami taste (glutamate) with bitter and umami receptors (T1R1 and T2R). The binding energies for the binding sites of the receptors were calculated *via* molecular docking simulation and validated *via* molecular dynamics simulation. As expected, bitter ligands have high affinity for T2R, and umami ligands have high affinity for T1R1. We build an affinity matrix (the "taste matrix") P_{ij} and discuss the dimensionality of the taste dataspace formed by these ligands in analogy with the RGB color vision space. The redundancy among the taste receptors can be treated mathematically as a linear dependency of columns and rows in the ligand–receptor interaction matrix, which we call the "taste matrix." We suggest a formula, $D = \mathrm{rank}(P_{ij})-1$, for the dimensionality of this taste dataspace (the number of linearly independent columns and rows) and calculate $D = 3$ for the taste determined by T1R1 and T2R. Given that bitterness forms a 2D dataspace, this result is consistent with the notion that umami taste is orthogonal to bitterness.

Received 8th January 2026
Accepted 2nd March 2026

DOI: 10.1039/d6ra00211k

rsc.li/rsc-advances

1. Introduction

The sense of taste detected by the human gustatory system is a regulator of feeding behavior. Since ancient times, primary tastes have been identified in European cultures. Aristotle wrote about two primary tastes and their variations, a total of eight tastes: "The species of flavor are, as in the case of color, simple, *i.e.*, the two contraries, the sweet and the bitter, and secondary, that is, on the side of the sweet, the oily, on the side of the bitter, the salty, between these come the pungent, the rough, the astringent, and the sour".[1]

Until the end of the 20th century, physiologists in Western countries believed that there were only four basic tastes: sweet, bitter, salty, and sour. The fifth sense, umami (Japanese 旨味, literary, "delicious taste") or savory, was suggested in 1907 by Japanese chemist Kikunae Ikeda. He coined the word "umami" and reported that Monosodium glutamate (MSG), a sodium salt of glutamic acid (Amino Acid notation: Glu or E), is responsible for this taste. By the beginning of the 21st century, umami had been widely recognized as the fifth primary taste. Umami is relevant to various food products, including wine [2–4] one of the most studied objects of taste perception. In addition to MSG, the umami taste is created by various nucleotides, amino acids (AAs), proteins, and peptides.[5]

There are also attempts to identify additional primary tastes, which appear occasionally in the scientific literature. Thus, since the 1990s, the calcium-sensing receptor (CaSR) has been a receptor for the kokumi (Japanese コク味 "rich taste") taste.[6,7] Recently, it has been suggested that starchiness (the taste of starch and other glucose oligomers) can be sensed independently of sweet receptors[8] and that ammonium chloride can be sensed by OTOP1 receptors.[9]

Human gustatory perception is complex and is mediated by several distinct classes of taste receptors and taste receptor cells. Thus, the salty taste is detected *via* several mechanisms, one of which is thought to rely on the sodium channel ENaC.[10] Sour-sensing cells are defined by the expression of PKD2L1 and OTOP1 ion channels,[11] whereas gustatory responses to carbonation are mediated by the membrane-tethered carbonic anhydrase CA IV.[12]

Specialized taste receptors called TAS (or just T) receptors are more complex. They form two families: the TAS1R (T1R) and TAS2R (T2R) families. Sweet and umami compounds are sensed by T1R heterodimers [13–15] whereas bitter compounds activate T2R receptors.[16–18] There are several dozen T2R receptors, 27 of which are listed in some studies.[19] Sweet taste is detected by the T1R2 + T1R3 heterodimer. The umami receptors are the T1R1 + T1R3 heterodimer receptors that respond to Glu and MSG and are metabotropic glutamate receptors, or mGluRs.

[a]*Infochemistry Scientific Center, ITMO University, 9 Lomonosova St., St. Petersburg, 191002, Russia. E-mail: nosonovsky@infochemistry.ru*

[b]*V.M. Gorbatov Federal Research Center for Food Systems of Russian Academy of Sciences, 26, Talalikhina str, 109316, Moscow, Russia*

[c]*College of Engineering and Applied Science, University of Wisconsin-Milwaukee, Milwaukee, WI 53211, USA. E-mail: shityakoff@hotmail.com*

The extracellular structural domain of T1R1, also called the Venus flytrap domain, acts as an orthosteric binding site and recognizes common umami substances, including peptides, amino acids, and nucleotides.[20] Both the umami receptor Venus flytrap domain (T1R1/T1R3-VFD) and the bitter receptor (*e.g.*, T2R14) often serve as protein receptors for docking in the identification of peptides with umami/bitter taste.[21]

Various attempts to catalog umami-tasting peptides have been made. Thus, Wang *et al.*[22] analyzed 205 umami peptides with 2–18 amino acids (AAs). Their results revealed that peptides with 2–3 amino acids account for 44% of the total umami peptides, and residues D and E are the key active sites, regardless of where they are in the peptides.[22] Later, Cui (2023)[21] studied 489 peptides with umami/bitter tastes from TPDB (https://tastepeptides-meta.com/) that were collected and used to train classification models on the basis of docking analysis, molecular descriptors (MDs), and molecular fingerprints (FPs) *via* five machine learning (ML) algorithms and four molecular representation schemes.[21] Charoenkwan *et al.* (2020; 2022) developed the iUmami-SCM database.[23,24] Ashikhmina *et al.* identified 774 oligopeptides (with lengths of 2–20) relevant to umami and reported that D, E, P, and G were the most common AAs.[5]

Building on prior efforts to characterize umami peptides and their sequence-driven taste determinants, a critical next step is to contextualize these molecular features at the level of taste receptor interactions. Bitter and umami perceptions are mediated by the closely related T2R and T1R receptor families, and increasing evidence suggests functional crosstalk between these pathways, motivating a unified exploration of bitter-umami taste space. In this regard, wine constitutes an experimentally and conceptually suitable model system, as it contains a chemically diverse yet well-characterized ensemble of bitter polyphenols and umami-related compounds whose sensory effects are transduced by T2R and T1R receptors, respectively.[25–27] The receptors selected in this study were guided by biological relevance, representativeness within the human T2R family, and the availability of structural information.[28,29] Specifically, T2R1, T2R30, and T2R46 are among the most extensively studied bitter taste receptors, with accessible sequence data, validated ligand interactions, and previously reported homology models, making them well-suited for comparative docking analyses. Moreover, these receptors span distinct functional clusters within the T2R family, enabling coverage of receptor diversity while minimizing redundancy. Within the wine matrix, polyphenols such as catechin, epicatechin, and flavan-3-ol are primary contributors to bitterness and astringency, whereas glutamate and inosine-5′-monophosphate act as key modulators of umami perception in fermented beverages. The coexistence of chemically distinct ligands engaging orthogonal taste pathways thus makes wine an ideal system for probing the dimensional structure of bitter–umami taste space (Fig. 1). Accordingly, this study employs *in silico* molecular docking and molecular dynamics simulations to investigate the interactions between representative wine-derived ligands and T1R and T2R receptors.

2. Computational methods

2.1. Molecular docking simulation

Molecular docking simulations of the interaction of bitter and umami ligands with T1R and T2R receptors were performed using the ligands ($n = 5$) responsible for the bitter, umami, and bitter tastes downloaded from the PubChem Database *via* the Python script (Fig. 1). Flavan-3-ol is responsible for the bitterness of amarone wine according to ACS data.[30,31] The script uses

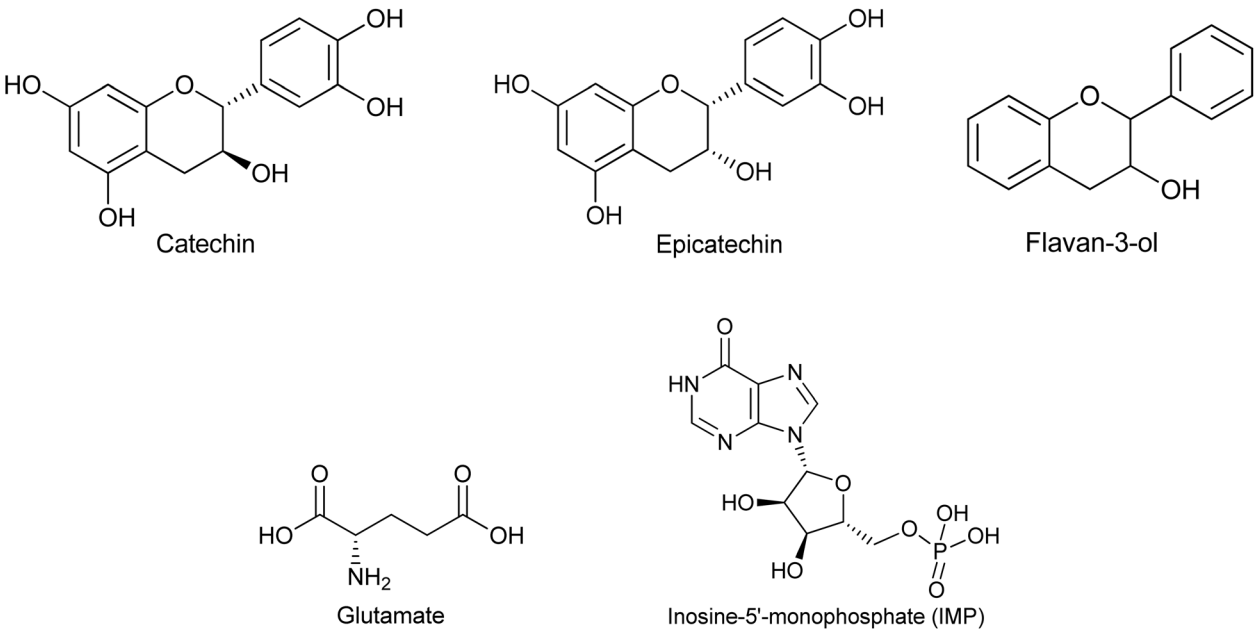

Fig. 1 Chemical structures of the five taste compounds used in this study.

the PubChemPy library to retrieve 3D chemical structures dynamically from the PubChem database for a list of specified compounds. The script then saves these structures in SDF (structure data file) format.

Protein structures for human taste receptors were retrieved from the AlphaFold Database using UniProt IDs. These structures were aligned in PyMOL against the TAS2R38 receptor as a reference model. Binding sites were predicted using the CASTp algorithm. Molecular docking was then performed with AutoDock v.4.2.6, implemented through the Raccoon pipeline for virtual screening. A standard genetic algorithm protocol (ga_run = 10) was employed for docking simulations, as previously described.[19] The binding affinity, expressed as Gibbs free energy (ΔG_{bind}), was calculated using the eqn (1):

$$\Delta G_{\text{bind}} = \Delta G_{\text{vdW}} + \Delta G_{\text{elec}} + \Delta G_{\text{HBond}} + \Delta G_{\text{tor}} + \Delta G_{\text{sol}} \quad (1)$$

where ΔG_{vdW} represents van der Waals nonbonded interactions between the ligand and receptor, encompassing both dispersion and repulsion forces; ΔG_{elec} accounts for coulombic (electrostatic) interactions between charged or partially charged atoms; ΔG_{HBond} describes hydrogen bonding interactions that stabilize the ligand–receptor complex; ΔG_{tors} reflects the torsional energy, which represents the entropic penalty associated with the flexibility of the ligand due to rotatable bonds; and ΔG_{sol} represents the desolvation energy, capturing the change in solvation energy when the ligand and receptor interact, including the energy associated with displacing water molecules from the binding site. Three-dimensional structural diagrams were prepared *via* PyMol.[32]

2.2. Taste modelling details

To describe taste perception within a low-dimensional mathematical framework, we adopt an analogy from sensory coding theory, where complex stimuli are represented through a limited number of receptor channels. Color vision provides a well-known example of such dimensionality reduction and serves here as a conceptual reference for organizing taste receptor-ligand interactions in a structured dataspace. In color vision, three cone photoreceptor types are tuned to short (S), medium (M), and long (L) wavelength light, corresponding approximately to blue, green, and red channels, respectively. This trichromatic coding provides a useful analogy for understanding how a small number of taste receptor pathways can combine to generate diverse taste qualities.[33–35]

For color vision perception, there are three types of cone cells and receptors, the S-, M-, and L-cells, which roughly correspond to blue, green, and red colors, respectively. The letters S, M, and L stand for short, medium, and long wavelengths, respectively. For light with a spectrum density of $\varphi(\lambda)$, where λ is the wavelength, the intensity of the mediated signal is given by eqn (2)

$$I_S = \int_0^\infty R_S(\lambda)\varphi(\lambda)d\lambda,\ I_M = \int_0^\infty R_M(\lambda)\varphi(\lambda)d\lambda,\ I_L = \int_0^\infty R_L(\lambda)\varphi(\lambda)d\lambda \quad (2)$$

where $R_S(\lambda)$, $R_M(\lambda)$, and $R_L(\lambda)$ are the corresponding responsivities of the receptors that reach their maxima in the short, medium, and long wavelength segments of the visible spectrum. Consequently, the continuous spectrum $\varphi(\lambda)$ is transformed into two signal intensity ratios (I_S/I_L, I_M/I_L), forming a 2D parameter space referred to as the "RGB space".[35]

It is much more difficult to characterize the taste space, although it has been suggested that 27 main bitter taste receptors form three clusters in the data space in terms of their interaction energies with bitter ligands; thus, similar to color vision, they can be characterized as a 2D space.[19] Similar to color vision, a mixture of substances can be presented as a vector of concentrations $C_n (1 \le n \le N$, where N is the total number of substances), whereas taste perception can be presented as a vector $I_m (1 \le m \le M$, where M is the total number of involved receptor types. The perception of the mixture is defined *via* matrix multiplication:

$$I_i = \sum_{j=1}^{N} P_{ij} C_j \quad (3)$$

where P_{ij} is the affinity matrix between ligands and receptors containing the sensitivity of the i-th receptor to the j-th substance. The elements of the matrix can be quantified as the binding energies between the i-th receptor and the j-th ligand. We call this a "taste space" matrix. The dimensionality of the taste space is defined by the number of linearly independent columns or rows in the matrix, which is equal to the rank of the matrix minus one

$$D = \text{rank}(P_{ij}) - 1 \quad (4)$$

Rank is the number of linearly independent vectors forming the rows of the matrix. The unity is subtracted since N points define the space of dimensionality of $D = N - 1$; thus, two points define a line, three points define a plane, *etc.*

To calculate the determinant, we further substitute $P_{ij} = 1$, the elements that provide good binding, with $\Delta G_{\text{bind}} < -6.0$ kcal mol^{-1}. The determinant of the 5×5 matrix given in Table 1 is $det(P_{ij}) = 0$, which automatically means that rank$(P_{ij}) < 5$. This is because the last two columns in the matrix are proportional. One can construct a 4×4 submatrix with a nonzero determinant by removing the last column and the fourth row as

$$det\begin{pmatrix} 0 & 0 & 0 & 1 \\ 1 & 0 & 1 & 0 \\ 1 & 1 & 1 & 0 \\ 0 & 0 & 1 & 0 \end{pmatrix} = 1 \quad (5)$$

Table 1 Reconstructed 'taste matrix' for five receptors and five ligands using the ΔG_{bind} value as a scoring function in kcal mol^{-1}

Receptor	Catechin	Epicatechin	Flavan-3-ol	Glutamate	IMP
T1R1	−5.8	−5.6	−5.5	−7.5	−5.9
T2R46	−6.1	−5.5	−6.1	−4.4	−5.7
T2R30	−6.5	−6.3	−6.3	−4.3	−5.8
T2R1	−7.3	−7.5	−6.7	−4.4	−5.6
T2R38	−5.7	−5.8	−6.2	−5.8	−5.9

We can conclude that the rank of the taste matrix is rank(P_{ij}) = 4.

2.3. Molecular dynamics simulation

To investigate the interactions of flavan-3-ol and glutamate with the receptors T1R1 and T2R38, receptor–ligand complexes were further investigated *via* MD simulations. Each complex was solvated within a rectangular box of TIP3P water molecules with 10 Å separation between any protein atom and the edge of the box to avoid edge effects. Counterions (Na^+ or Cl^-) were incorporated to neutralize the system charge. The protein and ligand were parameterized with the GAFF2 and AMBER ff19SB force fields, respectively, and water molecules were parameterized *via* the TIP3P model.

While T1R1 and T2R38 are membrane-associated receptors, and the inclusion of an explicit phospholipid bilayer would provide a more physiologically representative environment, in the present study, the MD simulations were intentionally conducted in an explicit aqueous environment to focus on the time-dependent stability of the ligand–receptor complex, including binding persistence, key intermolecular interactions, and local conformational fluctuations within the binding site. This simplified setup has been widely employed in comparative and screening-oriented MD studies, where the primary objective is to assess relative binding stability rather than full membrane-coupled receptor dynamics.

System topologies and coordinates were created *via* the LEaP module of AMBER22. Minimization was performed at 100 000 steps to relax water molecules and ions with the restrained protein–ligand complex.[36,37] Stepwise equilibration was subsequently performed at a constant volume (NVT ensemble) with positional restraints on the protein and the ligand at 5 ns. After equilibration, the production step was performed at 500 ns using a 2 fs time step, with bonds containing hydrogen atoms constrained by the SHAKE algorithm. The long-range electrostatics were treated *via* the particle mesh Ewald algorithm and cut off at 10 Å from the nonbonded state. Using CPPTRAJ [38] trajectory analyses were employed to identify the structural stability and dynamic behavior of the receptor–ligand complexes. Root-mean-square fluctuation (RMSD) and root-mean-square fluctuation (RMSF) analyses were employed to quantify protein backbone stability and residue flexibility, respectively. The radius of gyration (R_g) was calculated to monitor protein compactness throughout the course of the simulation.[39] Finally, free energies were predicted *via* the MMGBSA/MMPBSA approach on the trajectories, resulting in quantitative estimates of the thermodynamic stability of the receptor–ligand complexes. The energies were calculated using the MMPBSA.py command and a Python script that generates free energies for each frame. A total of 10% of the frames were selected for the free energy calculations.[40] The results, along with the standard deviation, are presented in Table 2. In addition, dynamic cross-correlation maps (DCCM) were constructed to gain insight into the binding conformations of the complexes.

3. Results and discussion

3.1. Virtual screening of protein–ligand complexes

We selected receptor–ligand complexes that represent both physiological relevance and chemical diversity in taste perception. Flavan-3-ol, catechin, and epicatechin were chosen as representative bitter polyphenols found in wine, where they contribute to astringency and bitterness.[19] Glutamate and inosine-5′-monophosphate (IMP) are included as canonical umami ligands, with glutamate serving as the primary activator of T1R1/T1R3 and IMP known to synergistically enhance umami responses. On the receptor side, T1R1 was selected as the key umami receptor, whereas T2R46, T2R30, T2R1, and T2R38 were chosen as representative members of distinct T2R clusters identified previously.[19] We modeled T1R1 as a monomeric unit for feasibility, although functional umami recognition involves the T1R1/T1R3 heterodimer.[41] Similarly, only representative T2Rs from distinct clusters were used.

Table 1 presents the docking scores (kcal mol^{-1}) of catechin, epicatechin, flavan-3-ol, glutamate, and IMP across human taste receptors (T1R1, T2R46, T2R30, T2R1, and T2R38). None of the ligands interacted with T1R1, except glutamate, whose binding affinity was >−6.0 kcal mol^{-1}. Catechin, epicatechin, and flavan-3-ol do not bind strongly to bitter receptors (T2R46 and T2R38). Notably, IMP displayed the lowest affinities.

As shown in Fig. 2, binding motifs in receptor families were also explored. Catechin, epicatechin, and flavan-3-ol, which are all flavonoids, share repeated hydrogen bonding and hydrophobic contacts with residues in both the sweet (T1R1) and bitter (T2Rs) receptor binding sites. These contact modes highlight their dual modulatory activities, which are implicated in bitter perception and sweetness masking. Glutamate engages strongly with T1R1 through hydrogen bonding and electrostatic interactions, reflecting its canonical role as an umami ligand. Interestingly, it docks less snugly with T2Rs, which suggests its selectivity for umami signaling pathways. IMP makes extensive contact with polar residues, particularly in T1R1, which is consistent with its function as an umami enhancer. The interaction of the phosphate group with the positively charged residues, including arginine, supports this observation. These findings provide a molecular basis for dietary polyphenol and nucleotide modulation of taste and are important for

Table 2 Energy profiles of protein–ligand complexes obtained from MD simulation results in kcal mol^{-1}

Receptor	Glutamate (ΔG_{GB})	Glutamate (ΔG_{PB})	Flavan-3-ol (ΔG_{GB})	Flavan-3-ol (ΔG_{PB})
T1R1	−30.87 ± 2.66	−12.47 ± 7.11	0.41 ± 0.08	0.41 ± 0.09
T2R38	−22.57 ± 2.43	−8.32 ± 4.42	−21.90 ± 1.81	−5.56 ± 4.14

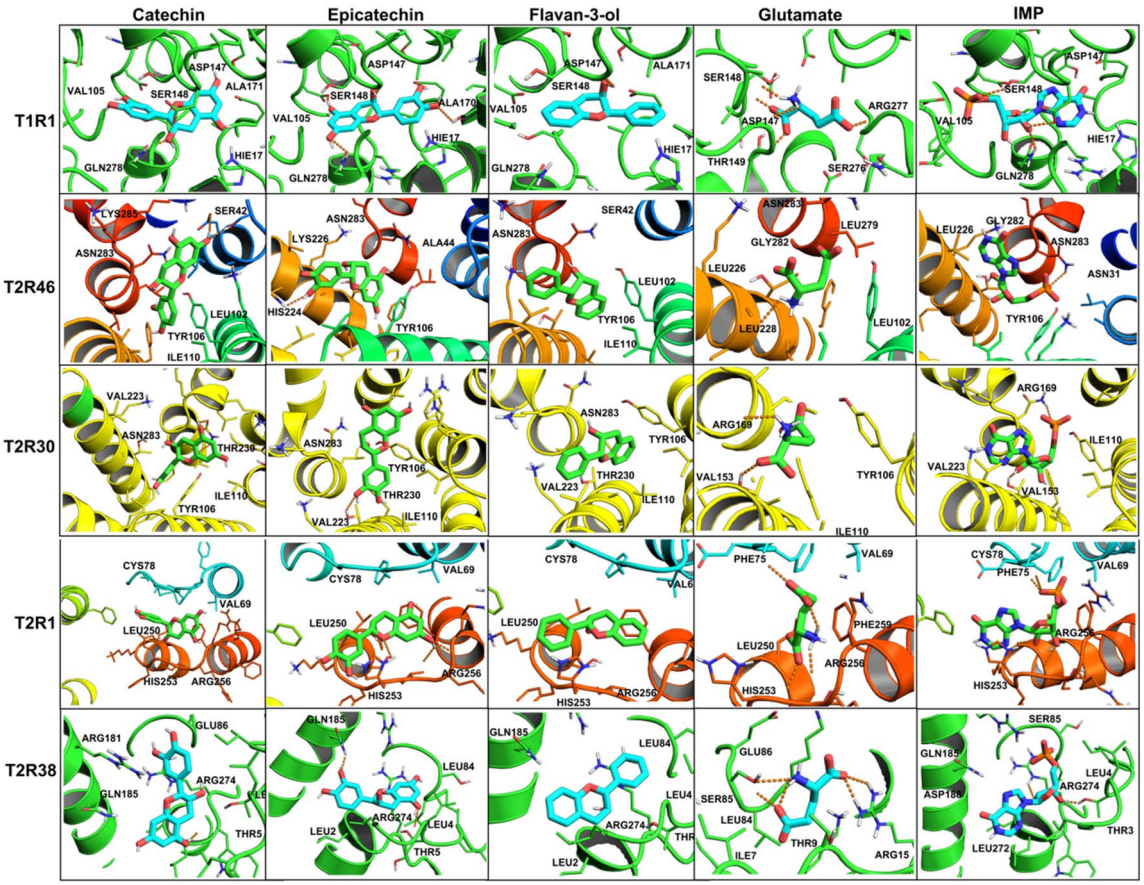

Fig. 2 Protein–ligand binding sites for five ligands—catechin, epicatechin, flavan-3-ol, glutamate, and inosine-5′-monophosphate—bound to five different taste receptors, T1R1, T2R46, T2R30, T2R1, and T2R38. Each panel highlights the binding site residues and ligand interactions within the receptor structures, displayed as colored ribbon helices with labeled amino acids.

nutritional therapies, functional food palatability, and therapeutic intervention for diet-associated diseases.

3.2. Dimension of the taste space

The interesting question of the dimension of the taste space can be treated by calculating the rank of the "taste matrix." Previously, we used clustering and principal component analysis to establish that bitter taste receptors tend to form three clusters (hence, a 2D data space).[19] Here, we use a different method based on the taste matrix. We can construct such a matrix, for example, for five receptors and five ligands, as shown in Table 1. A number of assumptions can be made. For ligands with binding energies of $\Delta G_{\text{bind}} > -6.0$ kcal mol^{-1} [42–44] it is assumed that no binding occurs, and the value of $P_{ij} = 0$ is taken. Some data are taken from Shityakov *et al.* (2025)[19] and Oliveira (2020).[45] For catechin and epicatechin, it is assumed that no docking with T1R1 occurs. For IMP, due to the absence of data, the value of $\Delta G_{\text{bind}} > -6$ was assumed. To further explore the interesting question of the dimensionality of the "taste space," docking data for another umami ligand, inosine-5′-monophosphate (IMP), with the bitter receptors T2R46, T2R30, and T2R1 were calculated as −6.3, −6.2, and −7.1, respectively (all $\Delta G_{\text{bind}} > -6.0$ kcal mol^{-1}). Notably, these three receptors represent three distinct clusters of T2R receptors, as reported by Shityakov *et al.* (2025).[19]

This means that the data space formed by T1R1 and T2R receptors is three-dimensional (eqn (2)). This is consistent with the observation by Shityakov *et al.* (2025) that the space of bitter receptors forms a 2D dataspace, given that the umami taste adds one additional dimension.[19] Note that the addition of the sweetness receptor (T1R2) and a sweet ligand (*e.g.*, sucralose) will likely add dimension to the taste matrix. The presentation of the ligand–receptor interaction in terms of the "taste matrix" helps to better understand the relationships between taste flavors, such as bitter, umami, and astringent flavors.

3.3. MD simulation

On the basis of the docking analysis, we selected four receptor–ligand complexes (glutamate and flavan-3-ol with T1R1 and T2R38) for molecular dynamics (MD) simulations to capture their biological relevance and contrasting binding behaviors. Glutamate is the primary physiological ligand of the canonical umami receptor T1R1, making this pair a natural benchmark for validating our workflow. In contrast, flavan-3-ol is a key wine-derived polyphenolic bitter compound, and T2R38 is a well-characterized bitter receptor previously established as

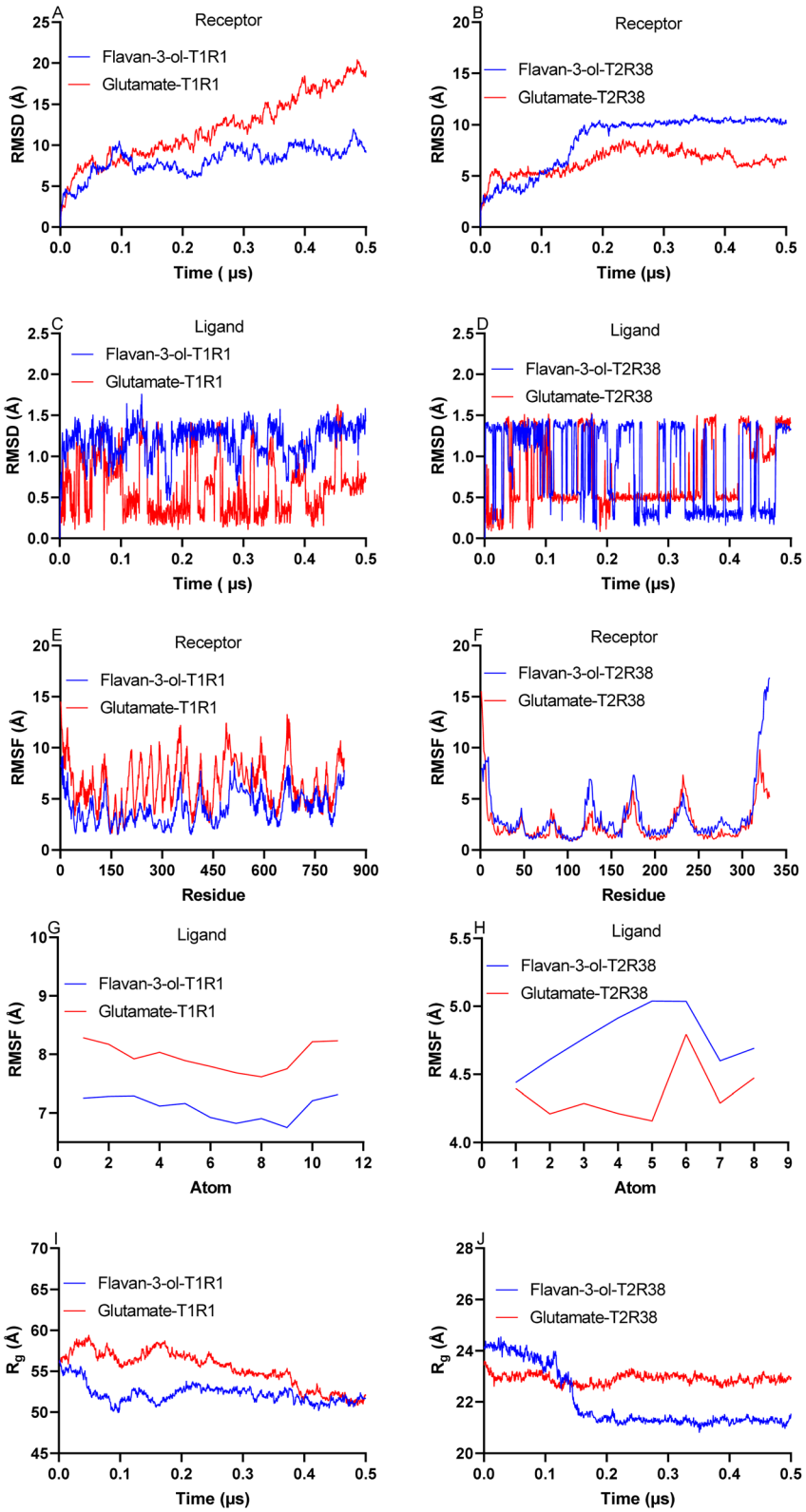

Fig. 3 Molecular dynamics (MD) simulations (500 ns) of T1R1 and T2R38 receptors with glutamate (solid line) and flavan-3-ol (dashed line). Panels: (A and B) receptor RMSD (Å); (C and D) ligand RMSD (Å); (E and F) receptor RMSF (Å); (G and H) ligand RMSF (Å); (I and J) radius of gyration (Å). Each metric illustrates the conformational dynamics and stability of the receptor–ligand complexes.

a reference in our earlier work.[19] Additionally, we were limited to T1R1 and T2R38 with glutamate and flavan-3-ol due to the high computational cost of MD simulations, excluding other T2R receptors (T2R46, T2R30, and T2R1) analyzed in docking studies. This focus on T2R38, a well-characterized reference receptor, may not fully capture the variability in binding dynamics across the T2R family, which consists of 27 receptors forming three clusters.[19] The exclusion of additional T2R receptors limits the generalizability of our findings to the broader bitter taste receptor family.

MD simulations provided insights into the stability and dynamics *via* the receptor RMSD (Fig. 3A and B), ligand RMSD (Fig. 3C and D), receptor RMSF (Fig. 3E and F), atom-by-atom ligand RMSF (Fig. 3G and H), and radius of gyration (Fig. 3I and J). For T1R1 with glutamate (Fig. 3A, C, E, G and I), the receptor RMSD and RMSF values revealed high conformational flexibility, with the ligand RMSD and RMSF values indicating dynamic reorientation and the R_g reflecting slight complex expansion, which was consistent with umami signaling. For T2R38 with glutamate and flavan-3-ol (Fig. 3B, D, F, H and J), the receptor RMSD and RMSF revealed a stable structure with restrained residue fluctuations, while the ligand RMSD and RMSF showed dynamic ligand reorientation, and the R_g confirmed compact complexes, reflecting the rigid binding environment of T2R38.

Following 500 ns MD simulations of glutamate and flavan-3-ol with T1R1 and T2R38 receptors, we performed free energy binding calculations with the MM/GBSA and MM/PBSA methods. The results, summarized in Table 2, elucidate the energetic contributions to ligand–receptor interactions, aligning with the molecular docking data from Section 3.1. Specifically, glutamate strongly binds to T1R1, with an MM/GBSA binding energy (ΔG_{GB}) of -30.87 kcal mol^{-1} and a Poisson–Boltzmann solvation energy (ΔG_{PB}) of -12.47 kcal mol^{-1}. These values reflect the extensive polar interactions of glutamate, particularly hydrogen bonding and electrostatic interactions, within the T1R1 binding site, enhancing complex stability. In contrast, flavan-3-ol binds weakly to T1R1 (ΔG_{GB} = 0.41 kcal mol^{-1}, ΔG_{PB} = 0.41 kcal mol^{-1}), suggesting that hydrophobic interactions dominate due to limited polar contacts.

For T2R38, flavan-3-ol has a comparable binding affinity (MM/GBSA) ($\Delta G_{GB} = -21.9$ kcal mol^{-1}) with glutamate ($\Delta G_{GB} = -22.57$ kcal mol^{-1}). Yet the MMPBSA results show that glutamate binds strongly ($\Delta G_{PB} = -8.32$ kcal mol^{-1}) than flavan-3-ol ($\Delta G_{PB} = -5.56$ kcal mol^{-1}). The favorable binding of flavan-3-ol

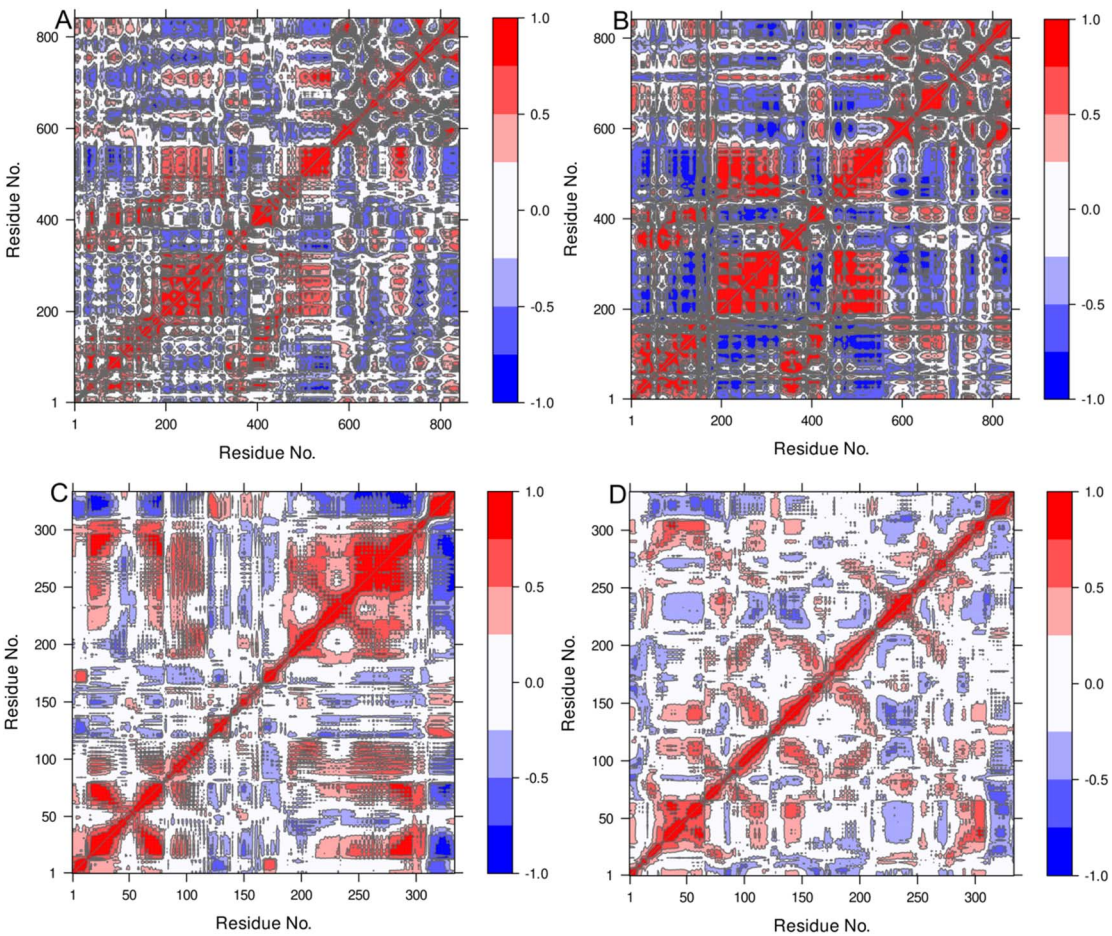

Fig. 4 DCCM of ligand–receptor interactions. (A) T1R1 with flavan-3-ol. (B) T1R1 with glutamate. (C) T2R38 with flavan-3-ol. (D) T2R38 with glutamate. Each plot illustrates residue–residue motion correlations, highlighting dynamic interactions between the ligands and receptors.

to T2R38 compared to T1R1 arises from robust hydrogen bonding and electrostatic interactions, which is consistent with its role as a bitter ligand. These trends suggest that glutamate is a potent agonist of T1R1-mediated umami signaling, whereas flavan-3-ol is a strong ligand for T2R38, modulating bitter taste perception.

Dynamic cross-correlation maps (Fig. 4) provide insights into residue–residue motion correlations for the receptor–ligand complexes. For T1R1 with flavan-3-ol (Fig. 4A), extensive positive correlations indicate cooperative residue motions, suggesting enhanced structural stability. Conversely, T1R1 with glutamate (Fig. 4B) shows pronounced anticorrelated motions between residue blocks, which is consistent with the role of glutamate as a canonical umami agonist that induces conformational rearrangements for signaling. For T2R38 with flavan-3-ol (Fig. 4C), broadly correlated motions reflect stabilized dynamics, reinforcing local and long-range interactions within the receptor. In contrast, T2R38 with glutamate (Fig. 4D) exhibited a mix of correlated and anticorrelated motions, indicating increased conformational flexibility. This flexibility suggests that glutamate promotes dynamic ligand recognition in T2R38 but lacks the stabilizing effect of flavan-3-ol.

4. Conclusion

We studied the molecular binding of umami and bitterness taste receptors with umami and bitter ligands, with an emphasis on those bitter ligands that are relevant to wine taste, since wine tasting is one of the most advanced areas of human taste studies. *In silico* molecular docking was verified *via* MD simulations. The large number of bitter taste receptors leads to redundancy (similar reactions of different receptors to the same set of ligands), which may be treated mathematically as a linear dependency of columns and rows in the ligand–receptor interaction matrix, which we call the "taste matrix."

We suggest a method to investigate the dimensionality of the taste perception space in the case of multiple types of taste receptors, such as T2R bitterness receptors and T1R1 umami receptors. We built an affinity matrix between bitter and umami ligands and bitterness and umami taste receptors (the "taste matrix") and found that the rank of the matrix is four, which corresponds to the 3D organization of the taste data space for these tastes. Umami taste perception is orthogonal to bitterness perception. This 3D organization was previously identified by clustering ligands' interactions with bitter taste receptors using principal components. Moreover, in the "taste space," sweetness perception (mediated by the T1R2 receptor) is orthogonal to bitterness perception, although it was not addressed in the present study. Understanding the organization of the taste space is important for the development of artificial taste analyzers ("artificial tongues").[46,47] Note that the present study is limited by its exclusive reliance on computational methods, which prevents direct biological validation of the predicted taste effects. Moreover, the dynamic nature of taste cannot be fully replicated by *in silico* models. To improve the reliability and applicability of the findings, future research should incorporate experimental approaches such as *in vitro* enzyme inhibition assays, cell-based receptor activation assays, and electrophysiological studies. These methods would enable experimental validation and refinement of the computational predictions, bridging the gap between theoretical models and biological reality.

Conflicts of interest

There are no conflicts to declare.

Data availability

The code and data used in this study are available in the GitHub repository at https://github.com/virtualscreenlab/TASR. This repository contains the source code used for the analysis, as well as the datasets utilized for training and testing the model. Researchers interested in replicating or extending this study can access the repository to review the code implementation and perform further analyses.

Acknowledgements

The research was carried out within the state assignment of Ministry of Science and Higher Education of the Russian Federation (project No.075-15-2024-483).

References

1 Aristotle. On the Soul. Translated by J. A. Smith. Accessed online 6/20/2025. https://classics.mit.edu/Aristotle/soul.2.ii.html.
2 D. Franceschi, G. Lomolino, R. Sato, S. Vincenzi and A. De Iseppi, Umami in Wine: Impact of Glutamate Concentration and Contact with Lees on the Sensory Profile of Italian White Wines, *Beverages*, 2023, **9**, 52, DOI: 10.3390/beverages9020052.
3 P. Klosse, Umami in wine, *Res. hosp. manag.*, 2013, **2**, 25–28, DOI: 10.1080/22243534.2013.11828287.
4 A. Vilela, A. Inês and F. Cosme, Is wine savory? Umami taste in wine, *SDRP J. Food Sci. Technol.*, 2016, **1**(3), 100–105, DOI: 10.25177/jfst.1.3.3.
5 M. S. Ashikhmina, *et al.*, Uncovering the taste features: Applying machine learning and molecular docking approaches to predict umami taste intensity of peptides, *Food Biosci.*, 2024, **62**, 105358, DOI: 10.1016/j.fbio.2024.105358.
6 Y. Ueda, M. Sakaguchi, K. Hirayama, R. Miyajima and A. Kimizuka, Characteristic flavor constituents in water extract of garlic, *Agric. Biol. Chem.*, 1990, **54**, 163–169.
7 Y. Maruyama, R. Yasuda, M. Kuroda and Y. Eto, Kokumi substances, enhancers of basic tastes, induce responses in calcium-sensing receptor expressing taste cells, *PLoS One*, 2012, **7**, e34489, DOI: 10.1371/journal.pone.0034489.
8 T. J. Lapis, M. H. Penner and J. Lim, Humans Can Taste Glucose Oligomers Independent of the hT1R2/hT1R3 Sweet Taste Receptor, *Chem. Senses*, 2016, **41**, 755–762, DOI: 10.1093/chemse/bjw088.

9 Z. Liang, C. E. Wilson, B. Teng, *et al.*, The proton channel OTOP1 is a sensor for the taste of ammonium chloride, *Nat. Commun.*, 2023, **14**, 6194, DOI: 10.1038/s41467-023-41637-4.
10 G. L. Heck, J. A. DeSimone and J. C. Skou, The epithelial sodium channel ENaC is a new target for aldosterone, *Kidney Int.*, 1984, **26**, 567–575.
11 A. L. Huang, X. Chen, L. D. Hwang, *et al.*, The cells and logic for mammalian sour taste detection, *Nature*, 2006, **442**, 934–938, DOI: 10.1038/nature05084.
12 J. Chandrashekar, D. A. Yarmolinsky, L. von Buchholtz, *et al.*, The taste of carbonation, *Science*, 2009, **326**, 443–445, DOI: 10.1126/science.1174605.
13 G. Nelson, M. A. Hoon, J. Chandrashekar, *et al.*, Mammalian sweet taste receptors, *Cell*, 2001, **106**, 381–390, DOI: 10.1016/S0092-8674(01)00451-2.
14 G. Nelson, J. Chandrashekar, M. A. Hoon, *et al.*, An amino-acid taste receptor, *Nature*, 2002, **416**, 199–202, DOI: 10.1038/416199a.
15 X. Li, L. Staszewski, H. Xu, *et al.*, Human receptors for sweet and umami taste, *Proc. Natl. Acad. Sci. U. S. A.*, 2002, **99**, 4692–4696, DOI: 10.1073/pnas.052599499.
16 J. Chandrashekar, K. L. Mueller, M. A. Hoon, *et al.*, T2Rs function as bitter taste receptors, *Cell*, 2000, **100**, 703–711, DOI: 10.1016/S0092-8674(00)80706-0.
17 K. L. Mueller, M. A. Hoon, I. Erlenbach, *et al.*, The receptors and coding logic for bitter taste, *Nature*, 2005, **434**, 225–229, DOI: 10.1038/nature03352.
18 W. Meyerhof, C. Batram, C. Kuhn, *et al.*, The molecular receptive ranges of human TAS2R bitter taste receptors, *Chem. Senses*, 2010, **35**, 157–170, DOI: 10.1093/chemse/bjp092.
19 S. Shityakov, E. V. Skorb and M. Nosonovsky, TAS2R taste receptor clustering suggests that bitter wine taste perception forms a 2D dataspace, *J. Comput. Biophys. Chem.*, 2025, **24**, 795–805, DOI: 10.1142/S2737416524500844.
20 M. Li, X. Zhang, Y. Zhu, *et al.*, Identifying Umami Peptides Specific to the T1R1/T1R3 Receptor via Phage Display, *J. Agric. Food Chem.*, 2023, **71**, 12004–12014, DOI: 10.1021/acs.jafc.3c02471.
21 Z. Cui, N. Zhang, T. Zhou, *et al.*, Conserved Sites and Recognition Mechanisms of T1R1 and T2R14 Receptors Revealed by Ensemble Docking and Molecular Descriptors and Fingerprints Combined with Machine Learning, *J. Agric. Food Chem.*, 2023, **71**, 5630–5645, DOI: 10.1021/acs.jafc.3c00591.
22 W. Wang, Z. Cui, M. Ning, *et al.*, In-silico investigation of umami peptides with receptor T1R1/T1R3 for the discovering potential targets: A combined modeling approach, *Biomaterials*, 2022, **281**, 121338, DOI: 10.1016/j.biomaterials.2021.121338.
23 P. Charoenkwan, J. Yana, C. Nantasenamat, *et al.*, iUmami-SCM: A Novel Sequence-Based Predictor for Prediction and Analysis of Umami Peptides Using a Scoring Card Method with Propensity Scores of Dipeptides, *J. Chem. Inf. Model.*, 2020, **60**, 6666–6678, DOI: 10.1021/acs.jcim.0c00707.
24 P. Charoenkwan, C. Nantasenamat, M. M. Hasan, *et al.*, UMPred-FRL: A New Approach for Accurate Prediction of Umami Peptides Using Feature Representation Learning, *Int. J. Mol. Sci.*, 2021, **22**, 13124, DOI: 10.3390/ijms222313124.
25 R. Gutiérrez-Escobar, M. J. Aliaño-González and E. Cantos-Villar, Wine Polyphenol Content and Its Influence on Wine Quality and Properties: A Review, *Molecules*, 2021, **26**(3), 718, DOI: 10.3390/molecules26030718.
26 D. Espinase Nandorfy, F. Watson, D. Likos, T. Siebert, K. Bindon, S. Kassara, R. Shellie, R. Keast and I. L. Francis, Influence of amino acids, and their interaction with volatiles and polyphenols, on the sensory properties of red wine, *Aust. J. Grape Wine Res.*, 2022, **28**(4), 621–637.
27 M. Behrens and W. Meyerhof, Bitter taste receptors and human bitter taste perception, *Cell. Mol. Life Sci.*, 2006, **63**(13), 1501–1509.
28 W. Xu, L. Wu, S. Liu, X. Liu, C. Zhou, J. Zhang, Y. Fu, Y. Guo, Y. Wu, Q. Tan and L. Wang, Structural basis for strychnine activation of human bitter taste receptor TAS2R46, *Science*, 2022, **377**(6612), 1298–1304.
29 L. Peri, D. Matzov, D. R. Huxley, A. Rainish, F. Fierro, L. Sapir, T. Pfeiffer, L. Waterloo, H. Hübner, Y. Peleg and P. Gmeiner, A bitter anti-inflammatory drug binds at two distinct sites of a human bitter taste GPCR, *Nat. Commun.*, 2024, **15**(1), 9991.
30 S. Soares, E. Brandão, C. Guerreiro, *et al.*, Tannins in Food: Insights into the Molecular Perception of Astringency and Bitter Taste, *Molecules*, 2020, **25**, 2590, DOI: 10.3390/molecules25112590.
31 M. Carrai, *et al.*, Association between taste receptor (TAS) genes and the perception of wine characteristics, *Sci. Rep.*, 2017, **7**, 9239, DOI: 10.1038/s41598-017-08946-3.
32 M. A. Lill and M. L. Danielson, Computer-aided drug design platform using PyMOL, *J. Comput. Aided Mol. Des.*, 2011, **25**, 13–19.
33 C. Spence and C. A. Levitan, Explaining crossmodal correspondences between colours and tastes, *i-Percept.*, 2021, **12**(3), 20416695211018223.
34 C. Spence, On the relationship (s) between color and taste/flavor, *Exp. Psychol.*, 2019, **66**(2), 99–111, DOI: 10.1027/1618-3169/a000439.
35 D. Purves, G. J. Augustine, D. Fitzpatrick, L. C. Katz, A. S. LaMantia, J. O. McNamara and S. M. Williams, *Cones and Color Vision. Neuroscience*, 2nd edn, Sinauer Associates, Sunderland (MA), 2001.
36 A. O. Owolabi, O. B. Akpor, J. A. Ndako, *et al.*, Antimicrobial Potential of Hippocratea indica Willd. Acetone Leaf Fractions against Salmonella Typhi: An In Vitro and In Silico Study, *Sci. Rep.*, 2024, **14**, 25222.
37 A. K. Oyebamiji, S. A. Akintelu, S. O. Afolabi, *et al.*, Computer Aided Study on Cyclic Tetrapeptide Based Ligands as Potential Inhibitors of Proplasmepsin IV, *Sci. Rep.*, 2025, **15**, 13865.
38 D. R. Roe and T. E. Cheatham, PTRAJ and CPPTRAJ: Software for Processing and Analysis of Molecular Dynamics

Trajectory Data, *J. Chem. Theory Comput.*, 2013, **9**, 3084–3095, DOI: 10.1021/ct400341p.

39 S. Shityakov, E. V. Skorb, C. Y. Förster and T. Dandekar, Scaffold Searching of FDA and EMA-Approved Drugs Identifies Lead Candidates for Drug Repurposing in Alzheimer's Disease, *Front. Chem.*, 2021, **9**, 736509, DOI: 10.3389/fchem.2021.736509.

40 S. O. Afolabi, E. O. Mensah, E. V. Skorb and S. Shityakov, Toxicity and Antiobesity Potential of Hunteria umbellata Compounds: A Computational ADMET and Binding Affinity Study. in *Silico Research in Biomedicine*, (2025) 100139, DOI: 10.1016/j.insi.2025.100139.

41 A. Goel, K. Gajula, R. Gupta and B. Rai, In-silico screening of database for finding potential sweet molecules: A combined data and structure based modeling approach, *Food Chem.*, 2021, **343**, 128538, DOI: 10.1016/j.foodchem.2020.128538.

42 S. Shityakov and C. Forster, In silico predictive model to determine vector-mediated transport properties for the blood–brain barrier choline transporter, *Adv. Appl. Bioinform. Chem.*, 2014, **7**, 23–36, DOI: 10.2147/AABC.S63749.

43 M. D. Khadem, S. Pirmoradi, M. R. Tabandeh, V. Zarezade and Z. Monjezi, In-silico identification of novel Cis-aconitate decarboxylase inhibitors as potential anti-inflammatory agents using molecular docking and dynamics, *Sci. Rep.*, 2025, **15**(1), 42412.

44 S. Hiremath, H. Kumar, M. Nandan, M. Mantesh, K. S. Shankarappa, V. Venkataravanappa, C. Basha and C. Reddy, In silico docking analysis revealed the potential of phytochemicals present in Phyllanthus amarus and Andrographis paniculata, used in Ayurveda medicine in inhibiting SARS-CoV-2, *3 Biotech.*, 2021, **11**, 44, DOI: 10.1007/s13205-020-02578-7.

45 M. S. Oliveira, Flexible Molecular Alignment: an Industrial Case Study on Quantum Algorithmic Techniques, Master's thesis, Universidade do Minho, 2020.

46 T. A. Aliev, V. E. Belyaev, A. V. Pomytkina, *et al.*, Electrochemical Sensor to Detect Antibiotics in Milk Based on Machine Learning Algorithms, *ACS Appl. Mater. Interfaces*, 2023, **15**, 52010–52020, DOI: 10.1021/acsami.3c12050.

47 L. M. Leidens, C. D. Boeira, M. H. Gonçalves, *et al.*, *ACS Appl. Electron. Mater.*, 2025, **7**, 5537–5548, DOI: 10.1021/acsaelm.5c00489.